THE ASTROPHYSICAL JOURNAL, 559:L37–L40, 2001 September 20

R AQUARII: EVIDENCE FOR DIFFERENTIAL ROTATION OF THE SiO MASER SHELL

J. M. HOLLIS,[1,2] D. A. BOBOLTZ,[3] J. A. PEDELTY,[4] S. M. WHITE,[2] AND J. R. FORSTER[5]

Received 2001 May 17; accepted 2001 August 8; published 2001 August 21

ABSTRACT

We previously reported Very Large Array and Berkeley-Illinois-Maryland Association (BIMA) array observations that suggested rotation of the SiO maser shell surrounding the long-period variable (LPV) in the R Aquarii binary system. In the present Very Long Baseline Array (VLBA) work, we report high spatial and spectral resolution observations of the $v = 1, J = 1–0$, SiO maser line that confirm our previous result and further suggest that the LPV maser shell is undergoing differential rotation. The 8–34 yr range of rotational periods resulting from differential rotation of the maser shell contains the ~18 yr period reported previously. The velocity structure of the VLBA data suggests a rotation symmetry axis oriented at a position angle of ~150°. The differential rotation model can be envisioned as a series of nested thin spherical shells that have a common rotation axis; each thin shell is characterized by its radius, r, with the innermost shell rotating fastest and the outermost shell slowest, in accordance with an equatorial plane velocity law of the form $v \propto (1/r^q)^{1/2}$. We find that $q \approx 1.09$ is necessary to approximate the VLBA data, suggesting that the differential rotation is approximately Keplerian.

Subject headings: circumstellar matter — masers — stars: individual (R Aquarii) — stars: rotation — stars: variables: other — techniques: interferometric

1. INTRODUCTION

R Aquarii is a symbiotic stellar system comprised of a mass-losing ~1–2 $M_\odot$ Mira-like long-period variable (LPV) with a 387 day period and an ~1.0 $M_\odot$ hot companion/accretion disk that is believed to give rise to the symmetrical jet seen at ultraviolet, optical, and radio wavelengths. The binary system orbit has been characterized as highly inclined to the line of sight (LOS; $i \sim 70°$) with large eccentricity ($e \sim 0.8$), has a semimajor axis of $\sim 2.6 \times 10^{14}$ cm, has an orbital period of ~44 yr, and lies at a distance of 200 pc (see Hollis, Pedelty, & Lyon 1997 and references therein). Hence, the northeast-southwest–oriented jet probably undergoes episodic refueling and subsequent increased activity at periastron since the hot companion passes through the outer envelope of the LPV. It is further posited that the binary system was at apastron circa 1996 (Hollis et al. 1997), so the LPV envelope would be little influenced by either the jet or the hot companion/accretion disk for many years near this epoch.

Recently, we (Hollis et al. 2000) conducted a multiepoch study (1996–2000) of the SiO maser shell that surrounds the LPV in the R Aqr binary system. Using data from moderate spatial resolution (~50 mas) Very Large Array (VLA) observations of $v = 1, J = 1–0$, SiO, and coarser spatial resolution (~300 mas) Berkeley-Illinois-Maryland Association (BIMA) array observations of $v = 1, J = 2–1$, SiO, we produced velocity maps that suggested the maser shell rotates with a period of ~18 yr. These velocity maps indicated that the western side of the maser shell is approaching and the eastern side is receding. This led us to suggest that the maser shell rotation axis is likely oriented approximately parallel to the direction of the northeast-southwest R Aqr jet. Constrained by conservation of angular momentum, we derived a minimum period of ~5 yr for the rotation of the LPV itself. Using corotation with the maser shell rotational period as a maximum, we concluded that the LPV rotational period would be constrained to a ~5–18 yr range. This range for the LPV rotational period, combined with an ~18 yr rotational period for the hot companion (Hollis & Koupelis 2000), prompted us to further conclude that tidal effects at successive periastron passages in the R Aqr binary system are tending to synchronize these stellar rotational periods to the orbital period of ~44 yr (Hollis et al. 1997).

Motivated by these successful VLA and BIMA array results, the present work was conducted to see what further can be determined from a high spatial resolution (~1 mas) Very Long Baseline Array (VLBA) study.

2. OBSERVATIONS

The $v = 1, J = 1–0$ SiO maser emission toward R Aqr ($\alpha = 23^h43^m51\overset{s}{.}693$, $\delta = -15°16'49\overset{''}{.}420$, J2000) was observed using the NRAO[6] VLBA on 2000 December 8 when the LPV was near minimum light at optical phase 0.43 (J. A. Mattei 2001, private communication). A line rest frequency of 43.122027 GHz was adopted. The data were recorded in dual circular polarization in a 4 MHz (27.8 km s^{-1}) band centered on a velocity of -26.0 km s^{-1} with respect to the local standard of rest (LSR). The setup was designed to produce 128 spectral channels with spacings of 31.25 kHz (~0.22 km s^{-1}). System temperatures and point-source sensitivities for each VLBA antenna in this frequency band are approximately 150 K and 11 Jy K^{-1}, respectively. The standard AIPS spectral line calibration and imaging procedure was used to produce an image cube containing images of spectral channels from -35.1 to -14.7 km s^{-1}. The resultant synthesized beam for the image cube is 0.85×0.45 mas at position angle [P.A.] = 1°. The nominal spatial resolution for the individual images is ~1 mas. In order to parameterize individual SiO maser spots in this

[1] Earth and Space Data Computing Division, Code 930, NASA Goddard Space Flight Center, Greenbelt, MD 20771.

[2] Department of Astronomy, University of Maryland, College Park, MD 20742.

[3] US Naval Observatory, 3450 Massachusetts Avenue, NW, Washington, DC 20392-5420.

[4] Biospheric Sciences Branch, Code 923, NASA Goddard Space Flight Center, Greenbelt, MD 20771.

[5] University of California at Berkeley; and Hat Creek Radio Observatory, 42231 Bidwell Road, Hat Creek, CA 96040.

[6] The National Radio Astronomy Observatory is a facility of the National Science Foundation operated under cooperative agreement by Associated Universities, Inc.

work, all emission features in each spectral (velocity) channel of the image cube with flux densities greater than 10 times the off-source 1 σ noise or 100% of the deepest negative were fitted with two-dimensional Gaussians to extract flux densities, positions, and sizes.

3. RESULTS AND DISCUSSION

The LOS velocity information derived from the VLBA data cube is shown in Figure 1. The top panel is a spectrum of the maser emission with color-coded LOS velocities that range from -34 to -16 km s^{-1}. Maser spots shown in the bottom panel are plotted in the same velocity color-coding that corresponds to the colors in the top panel spectrum. Since ~ -25 km s^{-1} is a reasonable LSR velocity for the R Aqr LPV (e.g., Lépine, Le Squeren, & Scalise 1978; Hollis et al. 1997), then it is apparent from Figure 1 that the blueshifted maser features predominantly lie on the southwestern region of the maser shell while the redshifted features lie to the northeast. Previous interferometric results with the VLA and BIMA array (Hollis et al. 2000) were similar, with blueshifted maser features lying to the northwest and redshifted features lying to the southeast. Taking both cases into consideration, a generally west-to-east rotation of the maser shell is strongly inferred, but the exact orientation of the rotational axis is yet to be determined. A long-term VLBA observing program may well be required to sort out the axis orientation due to the inherent unpredictable nature of maser shell emission. In any case, rotation of the maser shell surrounding the LPV in the R Aqr binary system has now been demonstrated (confirmed) with the present VLBA data.

Further investigation of the VLBA data cube showed that both the blueshifted features and, in turn, the redshifted features systematically moved in the same east-to-west direction on the sky as spectral channel images were viewed in sequence (i.e., from -34 to -16 km s^{-1}). Such systematic motion is characteristic of differential rotation. We were subsequently able to obtain a reasonable model of the LOS velocity structure of the VLBA data using the following form of differential rotation:

$$V(r)_{\rm LOS} = V_{\rm LPV} + \sqrt{\frac{G'M}{r^q}} \cos\theta \cos\phi \sin i, \qquad (1)$$

where, on the right-hand side, the first term is the LOS velocity of the LPV and the second term would represent the LOS velocity due to circular motion of the maser shell if and only if $q = 1$. In this instance, G' would equal the gravitation constant, G, in both units and numerical value. However, we considered a class of rotational velocity curves in which $q \neq 1$ and empirically found that only one value of $q \geq 1$ approximated the data when reasonable LPV masses were used in equation (1). In this instance, we retained the numerical value of G for G', but the units of G' change appropriately to preserve a dimensionally correct equation (1). Such an empirical approach with respect to this particular class of radial velocity profiles is not without precedent, having been used by Rosen et al. (1978) to gain insight into path lengths associated with OH and H_2O maser emission.

Our three-dimensional model can be envisioned as a series of nested infinitesimally thin spherical shells (hereafter the shell structure) that have a common rotation axis; visualization of this model is aided by referring to Figure 2. The size of each spherical shell is defined by its radius, r. Furthermore, as equation (1) indicates, the innermost shell would rotate fastest and the outermost shell slowest. In equation (1), the angle i is the inclination of the shell structure rotation axis to the LOS, the angle ϕ defines the latitudinal coordinate of the shell structure, and the angle θ is measured in the equatorial plane of the shell structure, where $\theta = 0°$ defines the east limb and $\theta = 180°$ the west limb of the maser shell structure as seen on the plane of the sky. The product $\cos\theta \cos\phi \sin i$ in equation (1) accounts for the LOS velocity due to rotation presented to the observer. As Figure 2 shows, each LOS through the maser shell structure will result in multiple rotation velocity components from emitting regions in all shells along the LOS having radii equal to or larger than that shell whose radius is tangent to the LOS. For example, LOSs near the limbs of the maser shell structure produce multiple LOS velocity components due to rotation that will be observed in addition to the ever-present $V_{\rm LPV}$ term (e.g., LOS 1 and LOS 3 in Fig. 2). For LOSs near the rotation poles (i.e., $\phi = \pm 90°$) and/or toward the middle of the shell structure (i.e., $\theta = 90°$ or 270°), a zero LOS velocity due to rotation results and, therefore, only $V_{\rm LPV}$ would be observed (e.g., LOS 2 in Fig. 2).

In order to approximate maser amplification path lengths in our three-dimensional model, we compute the LOS distance through the envelope at positions in which the LOS velocity due to rotation changes by less than the thermal velocity of the masing molecules. We estimate the SiO thermal line width

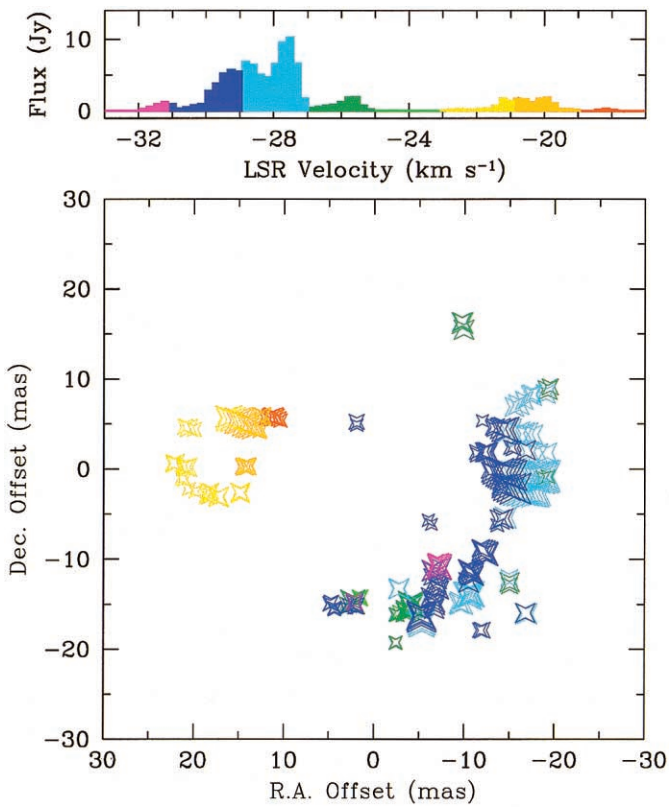

FIG. 1.—LOS velocity structure of the SiO maser emission toward the R Aqr LPV. *Top panel*: Spectral line profile plotted in color-coded velocity increments to show the progression of LOS velocities blueward (*left*) to redward (*right*) relative to $V_{\rm LPV} = -25$ km s^{-1}. *Bottom panel*: Spatial distribution of maser spots with color-coded velocities that match the increments in the top spectral line profile. The relative sizes of the symbols used for plotting maser spots are proportional to the natural logarithm of the flux densities for the maser spots. Maser spot position uncertainties are conservatively estimated to range between 3 and 146 μas.

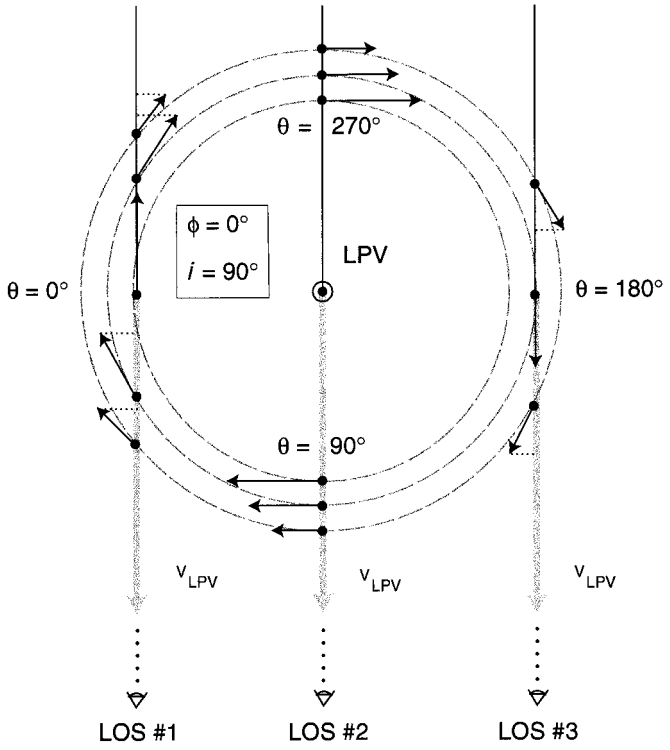

FIG. 2.—Schematic diagram of the differentially rotating SiO maser shell structure model. The idealized, not-to-scale diagram shows only the equatorial plane of the three-dimensional shell structure. LOS l (3) shows the east (west) limb LOS velocity components due to the approaching LPV and the receding (approaching) shell structure due to differential rotation in which the LOS component of the circular motion velocity vectors are projected onto the LOS as indicated by the dotted lines. Note that LOS l and LOS 3 are at slightly different radii. Along LOS 2 there is no LOS velocity component due to rotation, and only the approaching LPV motion is observable.

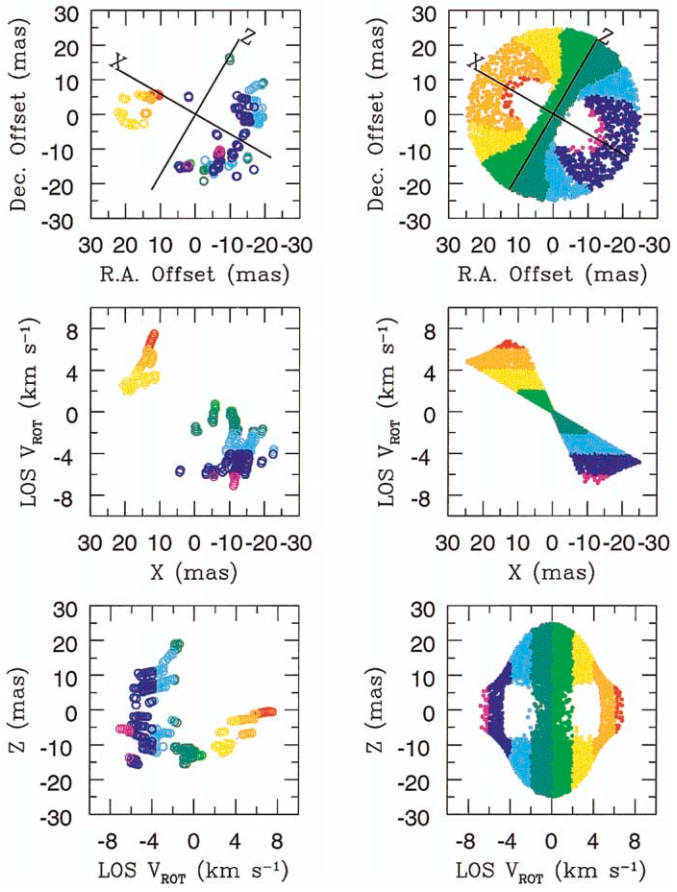

FIG. 3.—Side-by-side *rotational* velocity color-coded images of VLBA SiO data (*left*) and the differential rotation model (*right*). Rotational velocity color-coding is analogous to the top panel in Fig. 1 except that $V_{LPV} = -25$ km s^{-1} has been subtracted (e.g., light green represents 0–2 km s^{-1}, dark green represents 0 to -2 km s^{-1}, etc.). *Top panels*: Sky orientation of the VLBA data (*left*) and model (*right*) described in the text. Each panel shows the assumed rotational axis, *Z*, at P.A. = 150° and an orthogonal *X*-axis. The top left panel appears the same as the bottom panel in Fig. 1. *Middle panels*: LOS rotational velocity vs. *X* for the VLBA data (*left*) and the model (*right*). *Bottom panels*: LOS rotational velocity vs. *Z* for the VLBA data (*left*) and the model (*right*). While the model predicts that SiO maser emission directly toward the star and along the axis of rotation is theoretically possible, little or no emission is usually observed toward the center of these stars as is seen in the present observations. This suggests that there is enough of a velocity gradient in the maser shell beyond that contributed by differential rotation so that material that moves in a direction perpendicular to the LOS will provide optimal velocity coherence for a maser photon propagating outward (Elitzur 1982).

is $\leq$1 km s^{-1} for a temperature of 1300 K (Reid & Menten 1997). The computed path length was further constrained to be greater than the minimum path length of $\sim 10^{13}$ cm necessary for SiO maser emission (Elitzur 1982) and less than the physical LOS path length through the shell. The maser spot density that results from these path length calculations will be characterized by tangentially amplified SiO masers (i.e., as would be appropriate for longer tangential maser path lengths near the maser shell limb) as well as SiO masers comparably amplified in a narrowly confined region of the center of the maser shell. We subsequently describe the R Aqr model that is consistent with this global morphology.

For an LPV mass of 1.75 $M_{\odot}$, $i \sim 70°$, and $V_{LPV} = -25.0$ km s^{-1}, we find that $q \approx 1.09$ is necessary in equation (1) to approximate the VLBA data of R Aqr, which is assumed to be at a distance of 200 pc (Hollis et al. 1997). This was done in a "by eye" comparison of VLBA data and differential rotation model diagnostic images shown in Figure 3. The diagnostic images are color-coded rotational velocity images of VLBA data and the differential rotation model expressed by equation (1). To more clearly see the effects of rotation on the LOS velocity, we have omitted the ever-present V_{LPV} in constructing Figure 3 (cf. Fig. 1). The common origin of the maser shell coordinate systems (i.e., $\Delta\alpha$, $\Delta\delta$ and *X*, *Z*) shown in the top panels of Figure 3 was determined by a least-squares fit of a circle to the distribution of maser features as derived from the total intensity image cube. The fitted circle radius obtained was 16.3 mas. For modeling purposes, Figure 1 data suggest an outer shell radius of ~25 mas. Selecting an inner shell radius of 10 mas was guided by the 8.05 mas mean radius determination for the LPV itself from IR observations (van Belle et al. 1996). In accordance with equation (1) and a distance of 200 pc, the corresponding rotational periods for the 10 mas inner shell radius, the 16.3 mas fitted circle radius, and the 25 mas outer shell radius are ~8, ~18, and ~34 yr, respectively. The general direction of the rotation axis, *Z*, was initially influenced by the morphology of Figure 1 data (see also Boboltz, Diamond, & Kemball 1997) but, in the end, was determined to lie at P.A. ~ 150° by finding agreement between the data and model discriminators shown in the middle and bottom panels of Figure 3.

The limitations in comparing a phenomenon as sporadic and irregular as SiO maser emission in a single observing epoch are well known (see Elitzur 1992, p. 287), but the data and

model plots of LOS rotational velocity versus both X and Z shown in Figure 3 are highly suggestive of differential rotation. We found that the direction of the rotation axis, Z, could be varied by $\pm 10°$ and the mass of the LPV could range from 1.5 to 2.0 $M_\odot$ with little effect on these Figure 3 model plots. The mass range for the LPV is consistent with the 2.5–3.0 $M_\odot$ range usually assumed for the total mass of the binary system (see Table 2 of Hollis et al. 1997) as constrained by a ~44 yr binary period. However, q is highly constrained to be very near 1.09, suggesting approximate Keplerian motion. For example, values of 1.15 and 1.05 for q noticeably distorted the model plots to such a degree that they no longer approximated the VLBA data. It could well be that multiepoch VLBA data would fill in such plots and also permit the refinement of the geometry and physical parameters we have used in the employment of equation (1) and the construction of the model plots in Figure 3.

Given the model of differential rotation, one can obviously predict that maser spot radial velocities should systematically decrease within increasing distance from the maser shell center for the case of an LPV with a highly inclined rotation axis with respect to the LOS. Another consequence of differential rotation is that it reduces the path length for maser amplification in a turbulence-free maser shell. For example, in the case of solid-body rotation of the maser shell, the velocity component along the LOS at a particular impact parameter is constant (i.e., independent of the depth along the LOS) because the velocity increases when proceeding to larger radii, but this is compensated by the cos θ projection factor, which decreases when proceeding away from the tangent point (e.g., $\theta = 0°$ or 180°). In the case of approximate Keplerian rotation of the maser shell ($q \approx 1$), the velocity decreases when proceeding to larger radii along a given LOS, and the projection factor decreases as well, so the size of the zone around the tangent point is reduced where the projected velocity changes, say, by less than the thermal width of the maser line. In practice, turbulent motion in the maser shell complicates the straightforward interpretation of the consequences of differential rotation. In this work, we have been fortunate that the maser shell was relatively quiescent with respect to turbulence.

4. SUMMARY

Using the BIMA array and the VLA, Hollis et al. (2000) conducted a multiepoch (1996–2000) study of the R Aqr LPV in SiO emission, which suggested west-to-east rotation of the maser shell on the plane of the sky. From the resultant velocity structure, a rotational period of ~18 yr was determined for the maser shell. These earlier lower resolution spatial maps indicated that the orientation of the rotation axis was approximately northeast-southwest. Such an orientation would be consistent with the orientation of the jet in the system. Therefore, we naturally concluded in the earlier work that the rotation axis was in all probability oriented northeast-southwest.

In the present VLBA work, we have presented high spatial and spectral resolution VLBA observations of the $v = 1$, $J = 1$–0, SiO maser line that once again demonstrate (confirm) west-to-east rotation of the SiO maser shell surrounding the LPV in the R Aqr binary system. The much greater number of maser spots involved in the present work has permitted modeling of the maser shell to better discern the details of the rotation and its orientation. The velocity structure indicates a rotation symmetry axis lying at P.A. ~ 150°, and we suggest that this orientation may be refined as additional VLBA observations accumulate. These data further suggest that the LPV maser shell is undergoing differential rotation. In the course of this work, we constructed expanding and/or contracting outflow models but found such models were inconsistent with the observed velocity structure of the maser spot data. Thus, we found the simplest explanation is differential rotation with no concomitant expansion or contraction of the maser envelope. We developed a differential rotation model that can be envisioned as a series of nested thin spherical shells that have a common rotation axis; each thin shell is characterized by its radius, r, with the innermost shell rotating fastest and the outermost shell slowest, in accordance with an equatorial plane velocity law of the form $v \propto (1/r^q)^{1/2}$. We find that $q \approx 1.09$ is necessary to approximate the VLBA data, suggesting that the differential rotation is approximately Keplerian. The 8–34 yr range of rotational periods resulting from differential rotation of the maser shell contains the ~18 yr period reported previously (Hollis et al. 2000).

Our interferometric investigations of the R Aqr LPV in SiO emission during the last 5 years (1996–2001) span at least four pulsation cycles of the LPV. During this time, we have been fortunate to witness a relatively stable large-scale velocity pattern consistent with rotation, which is apparently independent of the LPV phase. Since the effects of rotation must be occurring at some level all of the time in LPVs (e.g., see Boboltz & Marvel 2000), observing the effects of rotation in an LPV like R Aqr, whose rotation axis is highly inclined to the LOS, is not surprising. Finally, an important general consequence of this work is that, mindful of the inherent unpredictable nature of SiO maser emission, one can test for the effects of differential rotation of the maser shell in other LPVs by the data-plotting method we have demonstrated here.

We thank an anonymous referee for a thorough reading of the manuscript and suggestions for improvement. J. M. H. gratefully acknowledges the hospitality of the University of Maryland, College Park, where he was a sabbatical visitor during the course of this study. J. M. H. and J. A. P. received support from NASA RTOP 344-02-03-01.

REFERENCES

Boboltz, D. A., Diamond, P. J., & Kemball, A. J. 1997, ApJ, 487, L147
Boboltz, D. A., & Marvel, K. B. 2000, ApJ, 545, L149
Elitzur, M. 1982, Rev. Mod. Phys., 54, 1225
———. 1992, Astronomical Masers (Dordrecht: Kluwer)
Hollis, J. M., & Koupelis, T. 2000, ApJ, 528, 418
Hollis, J. M., Pedelty, J. A., Forster, J. R., White, S. M., Boboltz, D. A., & Alcolea, J. 2000, ApJ, 543, L81
Hollis, J. M., Pedelty, J. A., & Lyon, R. G. 1997, ApJ, 482, L85
Lépine, J. R. D., Le Squeren, A. M., & Scalise, E., Jr. 1978, ApJ, 225, 869
Reid, M. J., & Menten, K. M. 1997, ApJ, 476, 327
Rosen, B. R., Moran, J. M., Reid, M. J., Walker, R. C., Burke, B. F., Johnston, K. J., & Spencer, J. H. 1978, ApJ, 222, 132
van Belle, G. T., Dyck, H. M., Benson, J. A., & Lacasse, M. G. 1996, AJ, 112, 2147